Doubly 1,3-Butadiyne-Bridged Ditwistacene with Enhanced Ultrafast Broadband Reverse Saturable Absorption

Yanbing Han,[a] Jinchong Xiao, *[b] Xingzhi Wu,[c] Yuxiao Wang,[a] Xueru Zhang,[a] and Yinglin Song *[a]

[a]Department of Physics, Harbin Institute of Technology, Harbin 150001, P. R. China. E-mail: ylsong@hit.edu.cn

[b]College of Chemistry and Environmental Science, Key Laboratory of Chemical Biology of Hebei Province, Key Laboratory of Medicinal Chemistry and Molecular Diagnosis, Ministry of Education, Hebei University, Baoding 071002, P. R. China. E-mail: jcxiaoicas@163.com.

[c]Jiangsu Key Laboratory of Micro and Nano Heat Fluid Flow Technology and Energy Application School of Mathematics and Physics, Suzhou University of Science and Technology, Suzhou 215009, P. R. China.

Content

Synthesis and Characterization

11,12-dibromo-2,7-di-tert-butyl-9,14-bis(4-(tert-butyl)phenyl)dibenzo[de,qr]tetracene (2)

A flask was charged with **1** (1.89 g, 3.0 mmol) and 2-amino-4,5-dibromobenzoic acid (944 mg, 3.2 mmol) in 1,2-dichloroethane (DCE, 20 mL). Followed by isoamyl nitrile (1 mL) under Ar. Then the reaction was gradually heated to 90 $^{\circ}$C and stirred overnight. After cooling to room temperature, brine was added and the mixture was extracted with methylene chloride. The organic layer was combined, dried over Na_2SO_4 and concentrated in vacuo. The residue was isolated via silica gel column chromatography (petroleum ether and methylene chloride as the eluent) to give the compound **2** (620 mg, 25 %) as a yellow solid. ^{1}H NMR (400 MHz, CDCl$_3$): δ = 8.17-8.15 (d, 2H), 8.09-8.10 (d, 2H), 7.84-7.85 (m, 4H), 7.52-7.56 (m, 4H), 7.42-7.45 (m, 4H), 1.41 (s, 18H), 1.10 (s, 18H). ^{13}C NMR (101 MHz, CDCl$_3$) δ = 150.57, 147.26, 138.40, 134.94, 131.97, 131.84, 131.33, 131.15, 130.30, 129.26, 127.59, 126.93, 126.57, 123.89, 122.64, 121.79, 34.82, 34.75, 31.54, 31.44.

((2,7-di-tert-butyl-9,14-bis(4-(tert-butyl)phenyl)dibenzo[de,qr]tetracene-11,12-diyl)bis(ethyne-2,1-diyl))bis(trimethylsilane) (3)

To a stirred solution of **2** (837 mg, 1.0 mmol, 1.0 equiv) and triphenylphosphine (26 mg, 0.10 equiv) in Et$_3$N, followed by CuI (20 mg, 0.10 equiv), Pd(PPh$_3$)$_2$Cl$_2$ (70 mg, 0.1 equiv) and (trimethylsilyl)acetylene (TMSA, 425 μL, 3 equiv) under Ar. Then the reaction mixture was heated to 85 $^{\circ}$C and stirred overnight. After cooling to room temperature, brine was added and the mixture was extracted with methylene chloride. The organic layer was combined, dried over Na_2SO_4 and concentrated in vacuo. The crude product was isolated via silica gel column chromatography (petroleum ether and methylene chloride as the eluent) to give the compound **3** (593 mg, 68 %) as a yellow solid. ^{1}H NMR (400 MHz, CDCl$_3$): δ = 8.12-8.11 (d, *J*=1.6 Hz, 2H), 8.06-8.05 (d, *J*=2.0 Hz, 2H), 7.84 (s, 4H), 7.59-7.57 (d, *J*=8 Hz, 4H), 7.47-7.45 (d, *J*=1.6 Hz, 4H), 1.43 (s, 18H), 1.12 (s, 18H), 0.30 (s, 18H). ^{13}C NMR (101 MHz, CDCl$_3$): δ = 150.73, 147.55, 139.00, 136.00, 132.38, 132.10, 131.68, 131.43, 130.63, 129.77, 127.92, 127.25, 126.79, 124.26, 122.90, 121.65, 104.64, 98.33, 35.18, 35.09, 31.91, 31.81, 0.51. MS (MALDI-TOF, m/z): calculated for C$_{62}$H$_{70}$Si2, 870.5016; Found, 870.5092.

2,7-di-tert-butyl-9,14-bis(4-(tert-butyl)phenyl)-11,12-diethynyldibenzo[de,qr]tetracene(4) Compound **3** (500 mg, 0.57 mmol, 1.0 equiv) was dissolved into the dried THF (20 mL), then 1.4 mL of 1 M TBAF in THF was added. After stirred for 2 h at the room temperature, brine methylene chloride was added, The organic layer was combined, dried over Na_2SO_4 and concentrated in vacuo. The residue was purified via silica gel column chromatography to afford the compound **4** (370 mg, 89 %). ^{1}H NMR (400 MHz, CDCl$_3$): δ = 8.14 (s, 2H), 8.12 (d, *J*=1.6 Hz, 2H), 7.85-7.84 (m, 4H), 7.58-7.56 (d, *J*=8.4 Hz, 4H), 7.48-7.45 (d, *J*=8 Hz,4H), 3.35 (s, 2H), 1.43 (s, 18H), 1.11 (s, 18H). ^{13}C NMR (101 MHz, CDCl$_3$): δ = 150.46, 147.25, 138.48, 135.66, 132.23, 131.94, 131.64, 131.09, 130.27, 129.31, 127.63, 126.91, 126.51, 123.91, 122.64, 120.18, 82.81, 80.60, 34.83, 34.74, 31.54, 31.45. MS (MALDI-TOF, m/z): calculated for C$_{56}$H$_{54}$, 726.4226; Found, 726.4227.

Synthesis of **DPDD**

Compound **4** (727 mg, 1 mmol, 1.0 equiv) was added into the suspension of Cu(OAc)$_2$·H$_2$O (4.0 g, 20 mmol) and CuCl (1.98 g, 20 mmol) pyridine (50 mL), then the reaction mixture was heated to 65 °C and stirred for 12 h. After cooling to room temperature, the solvent is evaporated via vacuo and the obtained residue was extracted with CH$_2$Cl$_2$ and brine. The organic layer was combined, dried over Na$_2$SO$_4$ and concentrated in vacuo. The crude product was isolated via silica gel column chromatography (petroleum ether and methylene chloride as the eluent) to obtain the compound **DPDD** (276 mg, 38%) as a yellow solid. ^{1}H NMR (400 MHz, CDCl$_3$): δ = 8.10 (s, 2H), 7.84-7.78 (d, 6H), 7.57-7.55 (d, *J*=8.0 Hz, 4H), 7.43-7.41 (d, *J*=8.0 Hz, 4H), 1.43 (s, 18H), 1.11(s, 18H). ^{13}C NMR (101 MHz, CDCl$_3$): δ = 150.54, 147.26, 138.28, 136.36, 132.33, 131.87, 131.35, 130.26, 129.19, 128.11, 127.58, 126.89, 126.57, 123.92, 123.75, 122.73, 92.63, 84.04, 34.83, 34.76, 31.55, 31.45. MS (MALDI-TOF, m/z): calculated for C$_{112}$H$_{104}$, 1449.8172; Found, 1449.8165. FT-IR (KBr): 3044, 2961, 2920, 2850, 2152, 1606, 1465, 1360, 1213, 879, 814 cm^{-1}.

Photophysical Measurements

One-photon photophysical measurement was obtained by using 10 mm pathlength spectroscopic quartz cuvette in DCM. UV-Vis absorption spectra was finished on a SPECORD 210 plus dual-beam spectrophotometer with DCM solvent as the baseline blank. Corrected steady-state emission was collected by a HITACHI (F-7000) spectrofluorometer. Fluorescence quantum yield was acquired at room temperature in air-saturated DCM using 9,10-diphenylanthracene in ethanol (Φ$_F$= 0.95) as a reference standard.
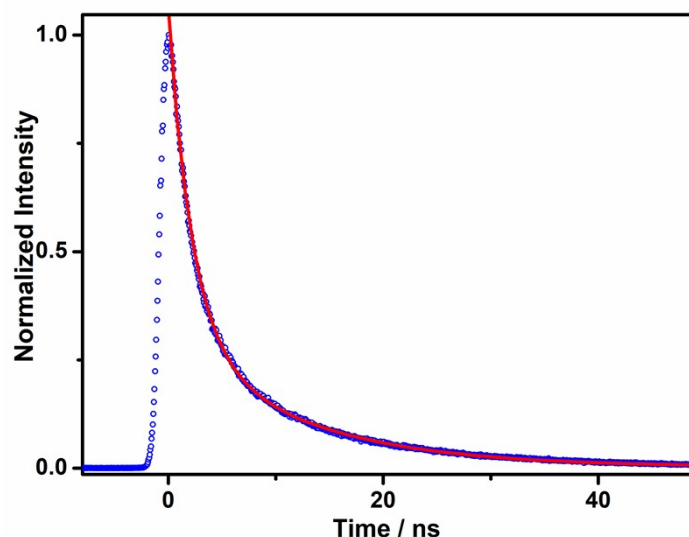
**Fig.S1** Fluorescence decay of **DPDD** in DCM.
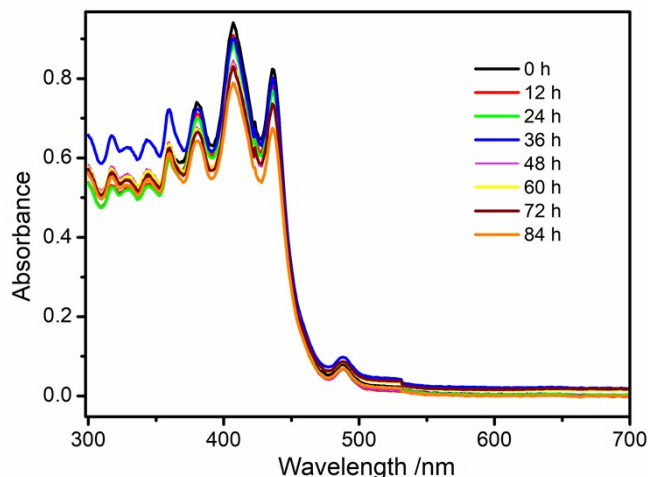
Fig. S2 UV-Vis absorption spectra of **DPDD** in DCM in different monitored time.
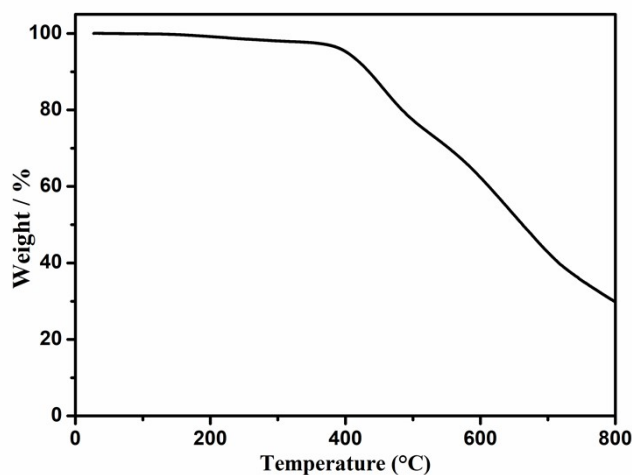
Fig. S3 TGA curves of **DPDD** under nitrogen. The heating rate is 10 °C/min.

Femtosecond transient absorption spectrum: The laser light source was produced by a regenerative amplified Yb:KGW fiber laser system (Light Conversion, PHAROS-SP), which produces a beam of laser with 1mJ pulses centered at 1030 nm with ~190 fs (FWHM) and the repetition rate of 6 kHz. The main part of this beam of laser was delivered to an optical parametric amplifier (OPA, ORPHEUS, Light Conversion) to produce the pump beam with tunable wavelength. The pump beam was set at 400 nm and modulated at 137 Hz using a chopper in this experiment. Another portion of the laser from the laser system pass through a computer-controlled optical translation stage (control delay time), then was focused into a 2 mm-thick sapphire crystal to generates a continuum white light as the probe beam. The probe signal was acquired by a rotating the grating inside the spectrometer, and the probe spectral region is between 470 to 1050 nm. The intensity level of the pump beam was carefully controlled below 12 mw to avoid photodegradation of sample during the course of the experiment. Sample was freshly dissolved in DCM in a 2 mm spectroscopic quartz cuvette for this measurement. The dynamics process was fitted throughout the global analysis using CarpetView analysis software.
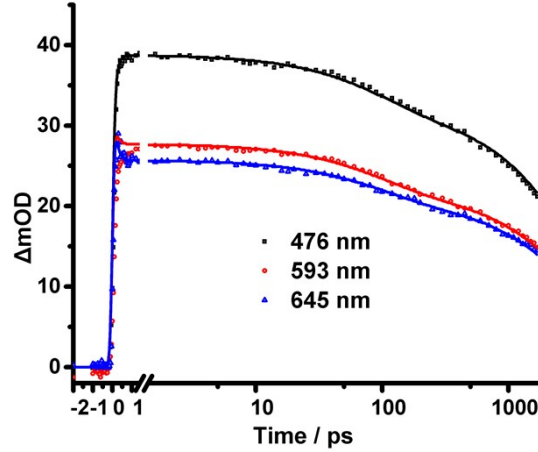
Fig. S4 Dynamics traces of selected wavelengths of 476 nm (black squares), 593 nm (red circles), and 645 nm (blue triangles) from femtosecond transient absorption spectrum. The dots represent the measured data and the solid lines are the numerical fitting with global analysis method.

Z-scans: open-aperture z-scan experiment under excitation with various pulse width was carried out to evaluate the nonlinear absorption ability of sample. The femtosecond laser light source is produced from an optical parametric amplifier (OPA, ORPHEUS, Light Conversion) with various wavelengths, picosecond laser pulses is from a Q-switched and mode-locked Nd:YAG laser with~21 ps (FWHM) at 532 nm, and ~4 ns (FWHM) pulses of 532 nm is obtained from a Q-switched Nd:YAG laser. The repetition rate for all pulse duration was set at 10 Hz to avoid nonlinearity from heat effect.[2] The laser beam was split two parts with a 50:50 beam splitter into two power detectors, which measured the laser pulse energy through the sample as a function of input laser pulse energy using an dual channel laser energy meter. The beam was focused using a lens with 250 mm focal length. A computer-controlled motorized translation stage offered millimeter movement along the z-axis. Sample was freshly prepared with a concentration of 0.15 mM in DCM and put into a 2 mm quartz cuvette for this measurement.

The z-scan data can be calculated to obtain nonlinear absorption coefficient by using the following equation[1]:

$$T(z) = \sum_{m=0}^{\infty} \frac{\left[-\beta_{eff} IL_{eff} / (1 + z^2 / z_0^2) \right]^m}{(m+1)^{3/2}} \tag{1}$$

Where β_{eff} is effective nonlinear absorption coefficient, I represents the incident intensity of laser. $L_{eff} = \left[1 - \exp\left(-\alpha_0 L \right) \right]/\alpha_0$ is the effective thickness of sample, α_0 represents the linear absorption coefficient of sample, z_0 and z represent the diffraction length of the laser beam and the propagation z-axis coordinate, respectively.

Based on mechanism of TPA and TPA-induced ESA, the nonlinear optical absorption coefficient can be presented as following equation:[2]

$$\alpha = \alpha_0 + \beta I + \gamma I^2 \tag{2}$$

Where β is the TPA coefficient, γ represents the three-photon absorption coefficient (TPA-ESA).

The fitting equation of TPA-ESA can be presented as following equation:

$$\frac{\mathrm{d}N_1}{\mathrm{d}t} = \frac{\sigma_0 N_0 I}{\hbar\omega} + \frac{\beta I^2}{2\hbar\omega} - \frac{N_1}{\tau_1} - \frac{\sigma_1 N_1 I}{\hbar\omega} + \frac{N_2}{\tau_2} \tag{3}$$

$$\frac{\mathrm{d}N_2}{\mathrm{d}t} = \frac{\sigma_1 N_1 I}{\hbar\omega} - \frac{N_2}{\tau_2} \tag{4}$$

$$N = N_0 + N_1 + N_2 \tag{5}$$

Where σ_0 and σ_1 is the ground state absorption cross section and the excited state absorption cross section of the sample, respectively; Ni ($i = 0,1,2$) represents the particle number density of S_0, S_1 and S_n states, τ_j ($j = 1, 2$) represents the lifetime of the corresponding energy level, $\hbar$ is the Planck constant, ω is the optical frequency. The β and γ can be obtained by fitting z-scan data using equations above, then TPA cross section σ_{TPA} is calculated by using equation:

$$\sigma_{\mathrm{TPA}} = \hbar\omega\beta/N \tag{6}$$

These procedures can effectively offer the corresponding nonlinear absorption coefficient, meanwhile establishes reliability of these parameter.
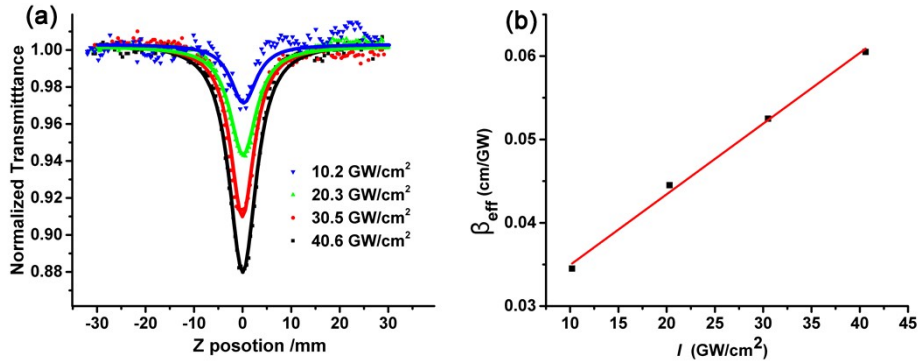

Fig. S5 Femtosecond open-aperture Z-scan data with the theoretical curve fitting at 532 nm with different incident powers; (b) Input laser intensity dependence of efficient nonlinear optical absorption coefficient.
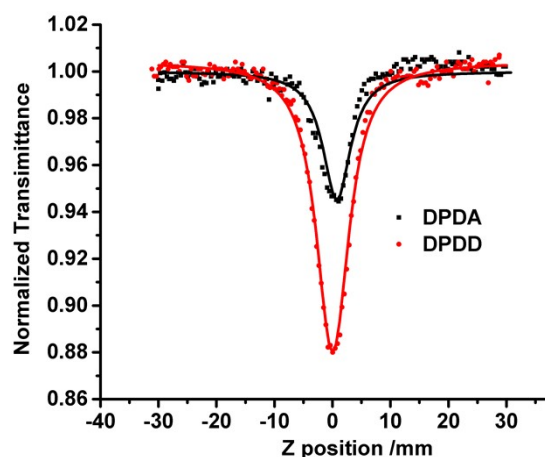
Fig. S6 Femtosecond open-aperture Z-scan response of **DPDA** vs **DPDD** after 532 nm excitation with a peak intensity of 40.6 GW cm^{-2} .

Table S1 The parameters of TPA and TPA induced ESA of **DPDA** vs **DPDD** at 532 nm and 540 nm achieved from Z-scan measurements.

		$\beta[10^{-2}cmGW^{-1}]$	σ_{TPA} [GM]	$\gamma[10^{-4} cm^3GW^{-2}]$
532 nm	**DPDA**	0.92	3850	0.35
	DPDD	2.31	9133	1.67
540 nm	**DPDA**	0.92	3312	0.49
	DPDD	2.63	9564	1.95
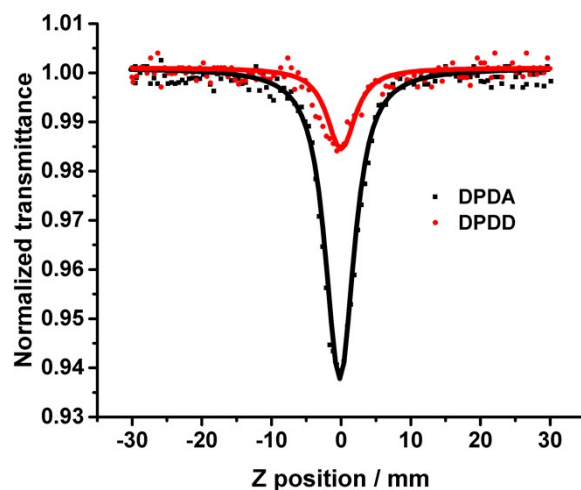
Fig. S7 Picosecond open-aperture Z-scan response of **DPDA** vs **DPDD** after 532 nm excitation with a peak intensity of 8.17 GW cm^{-2} .
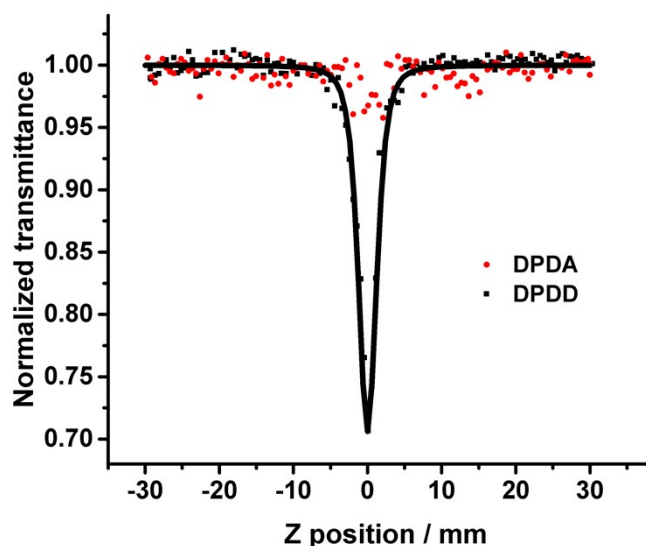
Fig. S8 Nanosecond open-aperture Z-scan response of **DPDA** vs **DPDD** after 532 nm excitation with a peak intensity of 3.48 GW cm^{-2} .

Table S2 The fitted parameters TPA induced ESA vaule for **DPDD** at 532 nm in various regimes.

	190 fs	21 ps	4 ns
γ [10^{-4} cm^{3}GW^{-2}]	1.95	21.55	2650

Two-Photon-Excited Fluorescence (TPEF) experiment: To further investigate two photon absorption, TPEE experiment was performed to measure TPA cross section for comparison with that from open-aperture z-scan experiment. The laser system for the TPA experiment was same with open-aperture z-scan experiment in the femtosecond regime. Pulse repetition rate was set at 6 kHz. The excitation wavelength was set in spectral region from 610 nm to 900 nm. The shorter wavelengths were not tested, which overlap with fluorescence signal. This overlap will interference the collection of fluorescence signal and result in a discrepancy between the experimental results and real results. The sample was put in the position of an unfocused femtosecond laser beam. In addition, the power of excitation beam was carefully controlled to avoid saturation of absorption and photodegradation of sample during the process of experiments. The TPA cross-sections are calculated by the equation[3]:

$$\delta_s = \frac{S_s C_r \Phi_r \eta_r}{S_r C_s \Phi_s \eta_s} \times \delta_r \tag{6}$$

where s and r represent the tested sample and standard reference sample, respectively. S represents the detected fluorescence integral area, C represents the concentration, Φ is the fluorescence quantum yield, η is the collection efficiency of instruments for this measurement. The fresh sample was contained into a 10 mm spectroscopic quartz cuvette, and every measurements for this two sample were carried out under the same experimental conditions. The standard reference sample is fluorescein aqueous with

pH11 for this experiment.

Calculation. The calculation was conducted using Gaussian 09 software package[4]. The ground states was optimized based on the density functional theory (DFT) with the B3LYP functional (DFT/B3LYP/ 6-31G(d, p)), and excited stated was calculated using the time-dependent density functional theory (TD-DFT) at the B3LYP/6-311G (d, p) level. After that, the Natural transition orbitals (NTOs) calculation was carried out to describe the electronic structure characteristics of electron and hole orbitals on the excited state. There are no imaginary frequencies based on frequency analysis, implying this large π-conjugated twistacences are closed-shell singlet state rather than open-shell diradical. The optimized structure shows double bridge model efficiently enforces planar conformation of the terminal part of side twistacene unit, and restricts the small rotational ability between side twistacene units.

Table S3 Optimized structure and Z-matrices (Å) of the ground state.
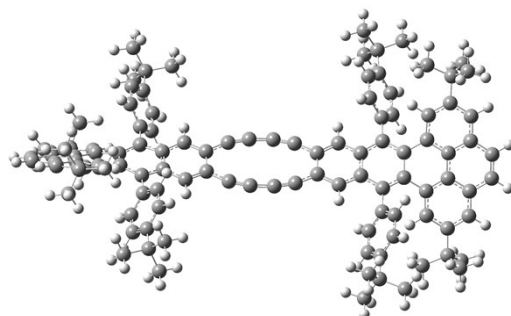
Optimized structure

C	5.57196	0.70165	0.09832	H	-8.4286	-2.42884	2.33112
C	5.56988	-0.71616	-0.12857	H	-12.70934	-2.39555	2.34347
C	4.31869	-1.39685	-0.12575	H	-13.9374	-0.94142	0.82561
C	3.11172	-0.73057	-0.05572	H	-13.94658	0.78725	-0.93307
C	3.11462	0.72787	-0.00124	H	12.43345	2.7817	4.54773
C	4.32405	1.38841	0.08156	H	11.42848	3.73288	5.64486
C	1.86046	1.39374	-0.01539	H	10.96052	2.07591	5.22379
C	1.85483	-1.39105	-0.0519	H	8.53589	4.34854	3.40369
C	0.66451	1.65481	-0.0322	H	8.6491	3.01123	4.56083
C	0.65731	-1.64468	-0.04149	H	9.25265	4.61393	4.99588
C	-0.69492	1.65852	-0.04804	H	10.65175	5.26072	2.2852
C	-0.70201	-1.64093	-0.02881	H	11.27657	5.6002	3.91087
C	-1.89288	1.40653	-0.06023	H	12.2473	4.66552	2.76316
C	-1.89749	-1.37806	-0.01543	H	11.00667	-2.12027	-5.18828
C	-3.14988	0.74567	-0.06268	H	12.4698	-2.8313	-4.49657
C	-3.15151	-0.71238	-0.00426	H	11.47292	-3.77906	-5.60406
C	-4.36021	-1.37384	0.08036	H	8.55482	-4.38314	-3.39264
C	-5.60821	-0.68807	0.09728	H	8.68503	-3.04659	-4.54883

C	-5.60878	0.729	-0.13115	H	9.28677	-4.65168	-4.9774
C	-4.3578	1.41072	-0.13321	H	10.65594	-5.30299	-2.25201
C	6.80483	1.36586	0.37391	H	11.29573	-5.64535	-3.87124
C	8.01017	0.64043	0.31028	H	12.25841	-4.71405	-2.71414
C	8.01062	-0.66737	-0.31094	H	-10.66466	5.30346	-2.24616
C	6.80255	-1.38677	-0.38877	H	-9.01765	4.81087	-2.65797
C	9.28263	1.11717	0.89821	H	-9.99939	5.68154	-3.84636
C	10.50219	0.517	0.48812	H	-12.42944	2.94597	-4.60898
C	10.50508	-0.55697	-0.45919	H	-12.67065	4.25906	-3.44039
C	9.28743	-1.1511	-0.88332	H	-11.91413	4.59106	-4.99932
C	9.33224	2.06587	1.93142	H	-10.03743	2.14938	-5.1675
C	10.5339	2.5074	2.50885	H	-9.65711	3.83346	-5.57069
C	11.72608	1.98969	2.00455	H	-8.64164	2.94716	-4.42946
C	11.73629	0.99806	1.01279	H	-10.59523	-5.27373	2.29813
C	11.74278	-1.04443	-0.96931	H	-11.24301	-5.61934	3.91377
C	11.73915	-2.03661	-1.96058	H	-12.21679	-4.722	2.73901
C	10.55034	-2.54902	-2.47809	H	-11.05956	-2.07538	5.20129
C	9.34428	-2.10099	-1.91506	H	-12.49587	-2.83287	4.50248
C	12.96787	0.45361	0.50984	H	-11.48503	-3.74205	5.62919
C	12.9711	-0.50591	-0.45225	H	-8.70667	-2.94739	4.59502
C	-6.83993	-1.35309	0.37509	H	-9.27285	-4.56218	5.03589
C	-8.04542	-0.62926	0.31222	H	-8.53057	-4.29388	3.45625
C	-8.05142	0.68049	-0.30639	H	7.98216	3.32228	-1.07725
C	-6.84352	1.39905	-0.38795	H	5.53171	2.74383	2.39688
C	-9.31528	-1.11696	0.89598	H	5.54692	-2.76397	-2.42408
C	-10.53937	-0.54272	0.46487	H	7.95347	-3.34469	1.08021
C	-10.54736	0.53087	-0.48175	H	-7.92067	3.36814	1.11801
C	-9.33255	1.15685	-0.88099	H	-5.62898	2.76415	-2.45835
C	-11.78457	0.98789	-1.01382	H	-8.01613	-3.31492	-1.07134
C	-11.79137	1.98533	-2.00549	H	-5.56359	-2.72521	2.39937
C	-10.61029	2.54086	-2.482	H	-7.7311	5.78624	0.83857
C	-9.40065	2.12112	-1.89286	H	-5.43925	5.18168	-2.7504
C	-9.35954	-2.05595	1.93711	H	5.41775	5.15689	2.72865
C	-10.56077	-2.51771	2.50108	H	7.8725	5.74247	-0.75444
C	-11.75516	-2.03196	1.97238	H	7.83528	-5.76524	0.76306
C	-11.77132	-1.04814	0.97192	H	5.42519	-5.17738	-2.75067
C	-13.00439	-0.53607	0.44306	H	-7.90267	-5.73417	-0.74323
C	-13.00926	0.41977	-0.52368	H	-5.44568	-5.13719	2.73636
C	10.57064	3.54735	3.64628	C	-6.388	7.21934	-1.1713
C	11.39983	2.99899	4.83169	C	-6.60524	-7.18211	1.19763
C	9.16646	3.89551	4.17395	C	6.55816	-7.21837	-1.18708
C	11.22784	4.84479	3.11812	C	6.57959	7.19655	1.18459
C	10.59496	-3.58977	-3.6145	C	-6.94875	7.642	-2.54951
C	11.43845	-3.04486	-4.79139	H	-6.44624	7.12408	-3.37151

C	9.19499	-3.93277	-4.15652	H	-8.01921	7.42504	-2.62197
C	11.24187	-4.88948	-3.07926	H	-6.80889	8.7182	-2.70112
C	6.76788	2.83856	0.63479	C	-7.11713	8.03448	-0.08679
C	6.76171	-2.85981	-0.64721	H	-6.73342	7.81634	0.91506
C	-6.79135	2.87291	-0.6436	H	-6.97027	9.10379	-0.26909
C	-6.80111	-2.82554	0.63852	H	-8.19528	7.84397	-0.09019
C	-10.58319	3.5911	-3.60877	C	-4.88106	7.56609	-1.10604
C	-10.02985	4.92445	-3.05397	H	-4.45513	7.28169	-0.13844
C	-11.98437	3.85528	-4.19185	H	-4.31143	7.0513	-1.8853
C	-9.67347	3.09769	-4.75877	H	-4.73212	8.64338	-1.2402
C	-10.59217	-3.54863	3.64685	C	-8.03768	-7.74343	1.35936
C	-11.2	-4.86883	3.11602	H	-8.52438	-7.32651	2.24718
C	-11.46214	-3.0152	4.80955	H	-8.66597	-7.5133	0.49408
C	-9.18999	-3.8506	4.20773	H	-8.0093	-8.83339	1.46872
C	7.42173	3.72295	-0.23806	C	-5.94943	-7.8083	-0.05631
C	7.35656	5.09921	-0.04745	H	-4.92855	-7.43663	-0.19117
C	6.63767	5.66742	1.01922	H	-5.90439	-8.89878	0.04188
C	5.98748	4.77987	1.88723	H	-6.51111	-7.57878	-0.96649
C	6.04763	3.39718	1.69917	C	-5.78324	-7.60178	2.4307
C	6.05135	-3.41785	-1.71851	H	-5.77119	-8.69336	2.51104
C	5.98664	-4.80078	-1.90349	H	-4.74352	-7.2658	2.36195
C	6.62205	-5.6891	-1.02538	H	-6.21029	-7.2076	3.35867
C	7.3311	-5.12143	0.04813	C	5.75054	-7.6415	-2.42841
C	7.40092	-3.745	0.23565	H	4.7111	-7.30195	-2.37442
C	-7.3785	3.76265	0.26392	H	6.1905	-7.25314	-3.35279
C	-7.2665	5.14424	0.09907	H	5.73596	-8.73342	-2.50362
C	-6.56475	5.70226	-0.97821	C	5.88434	-7.83622	0.06145
C	-5.99039	4.80334	-1.89439	H	4.86319	-7.46032	0.18166
C	-6.09509	3.42449	-1.73253	H	5.83664	-8.92699	-0.03214
C	-7.45423	-3.71282	-0.23181	H	6.43535	-7.60433	0.97753
C	-7.38705	-5.0886	-0.03809	C	7.99082	-7.78492	-1.32772
C	-6.66638	-5.65343	1.02917	H	8.4903	-7.37346	-2.211
C	-6.0169	-4.76296	1.8947	H	8.6088	-7.55306	-0.45549
C	-6.07927	-3.38079	1.70356	H	7.96025	-8.87525	-1.43265
H	4.30439	-2.47631	-0.19138	C	5.7593	7.62024	2.4174
H	4.31433	2.4679	0.1477	H	4.71893	7.28596	2.3501
H	-4.34954	-2.45314	0.14886	H	6.18635	7.22716	3.34584
H	-4.34373	2.48998	-0.20166	H	5.74924	8.712	2.49553
H	8.40401	2.46098	2.30954	C	5.92418	7.82153	-0.07014
H	12.68182	2.33496	2.38891	H	4.90248	7.45163	-0.2036
H	12.69756	-2.38668	-2.33384	H	5.88138	8.91229	0.0259
H	8.41856	-2.49193	-2.30354	H	6.48479	7.58911	-0.98025
H	13.90205	0.83949	0.90932	C	8.01334	7.75523	1.34421
H	13.90795	-0.89644	-0.8408	H	8.50002	7.33862	2.2322

| H | -12.75169 | 2.29772 | -2.40019 | H | 8.64044 | 7.52263 | 0.47873 |
| H | -8.48207 | 2.55458 | -2.25703 | H | 7.9872 | 8.8454 | 1.45204 |

Table S4 Values of energies, oscillator strengths and contributions of the respective molecular orbitals for S0→Sn.

State	Energy/ev	MO → MO contributions		Oscillator strength
S1	2.4653	HOMO-1→LUMO	45.1%	0.0207
		HOMO→LUMO+1	52.3%	
S2	2.4790	HOMO-4→LUMO+1	18.6%	0.0024
		HOMO-1→LIMO+1	61.5%	
		HOMO→LUMO	26.7%	
S3	2.6596	HOMO-1→LUMO+1	24.1%	0.0070
		HOMO→LUMO	64.3%	
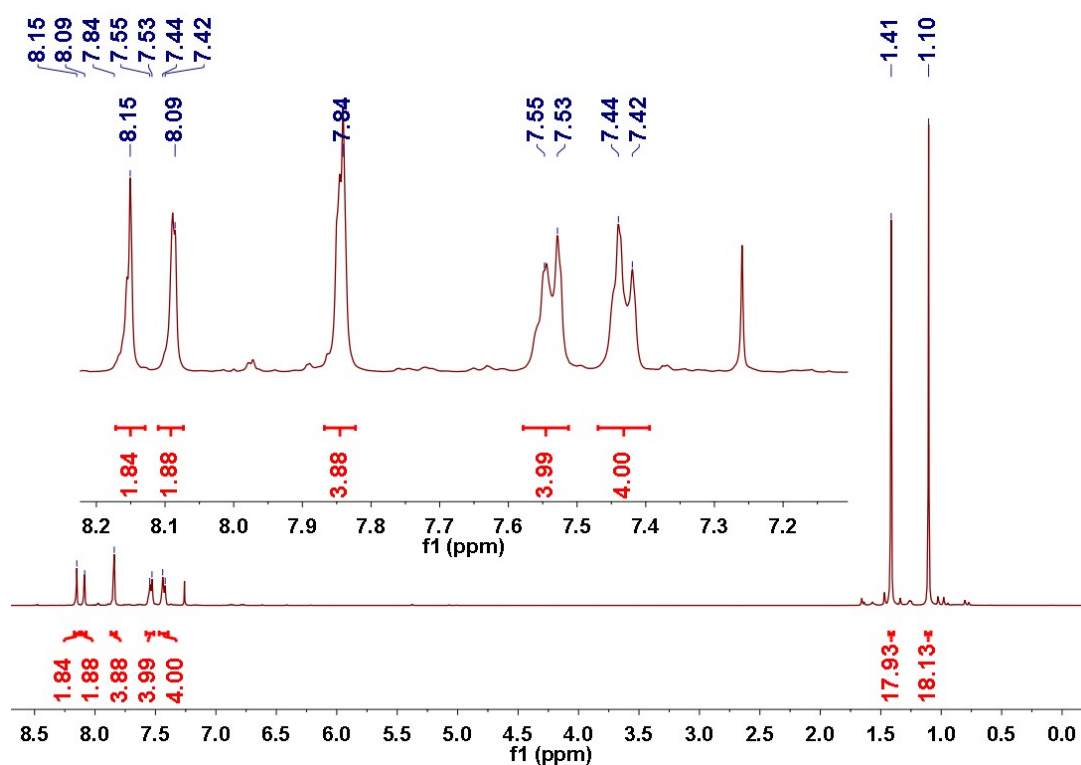
Fig. S9 ^{1}H NMR spectrum of **2**.
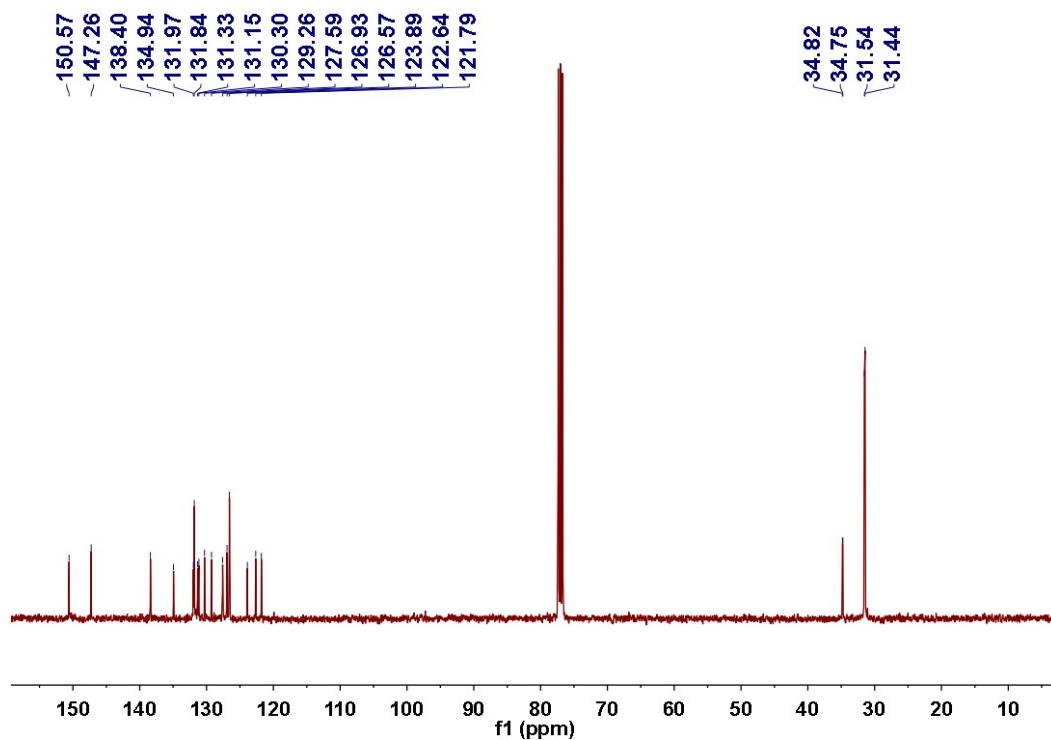
Fig. S10 ^{13}C NMR spectrum of **2**.
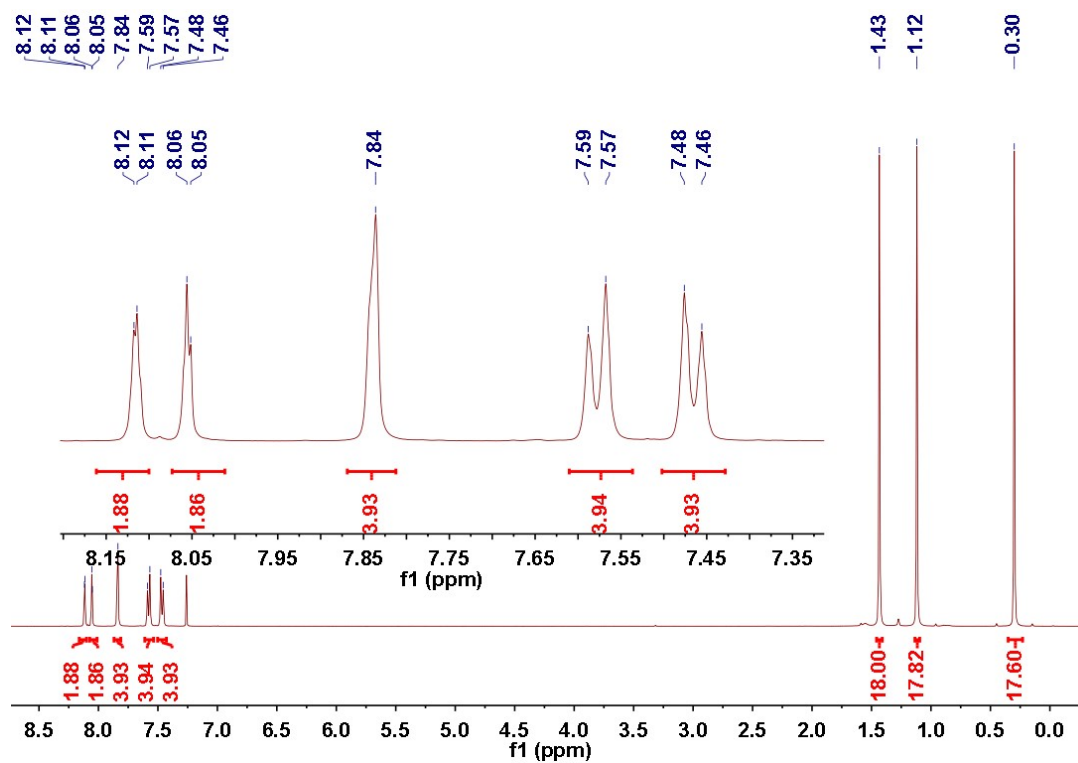
Fig. S11 ^{1}H NMR spectrum of **3**.
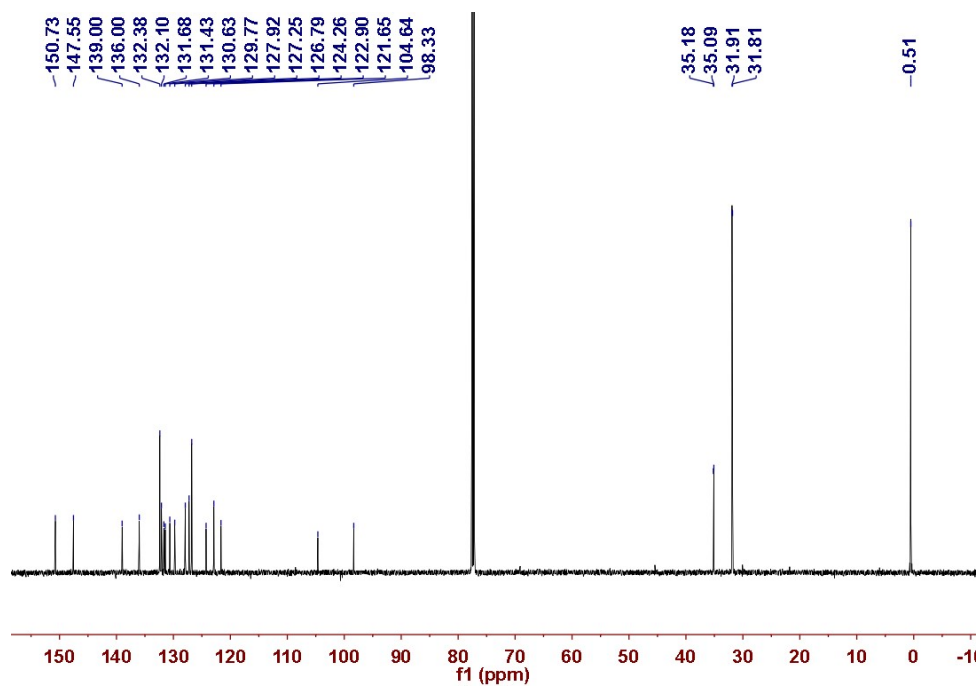
Fig. S12 ^{13}C NMR spectrum of **3**.
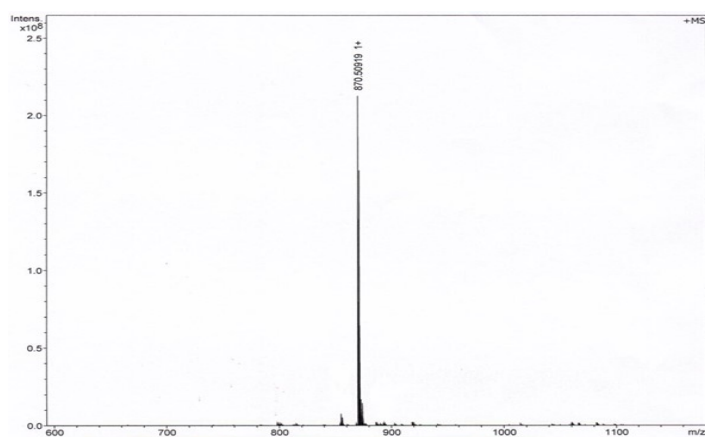
Fig. S13 MALDI-TOF spectrum of **3**.
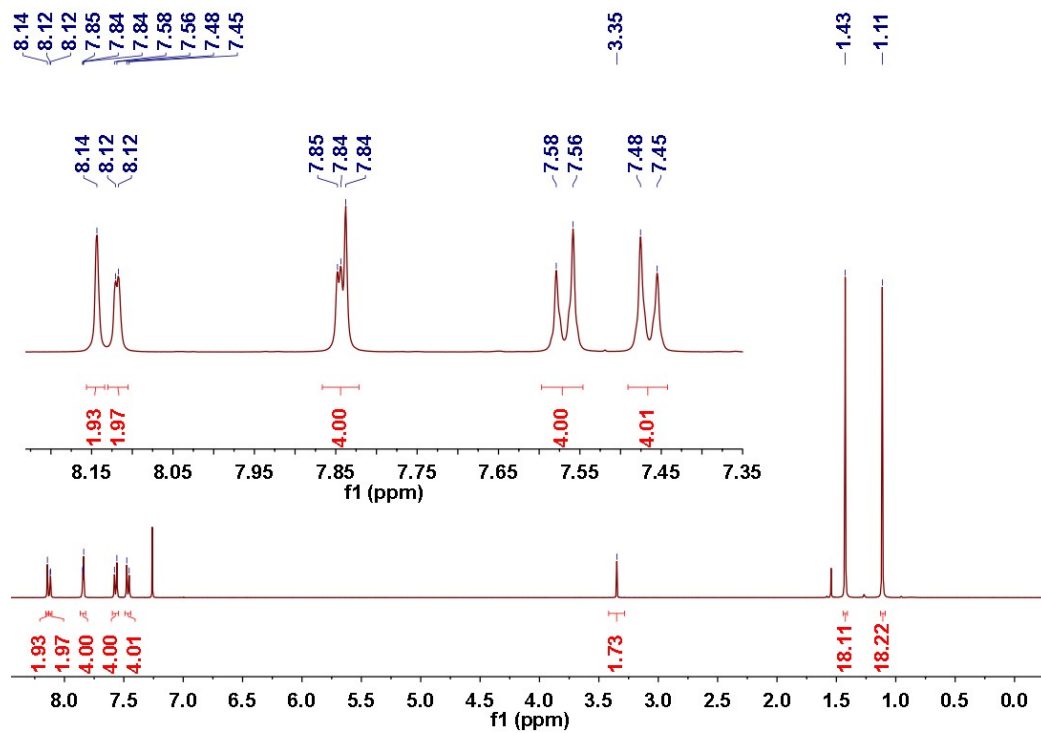
Fig. S14 ^{1}H NMR spectrum of **4**.

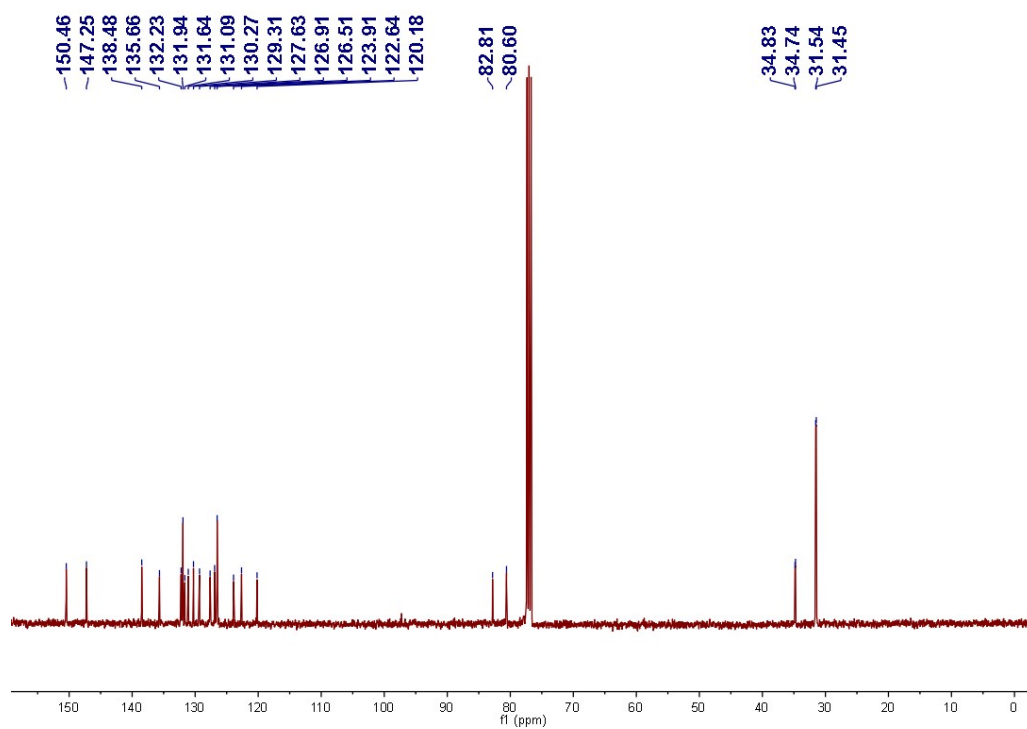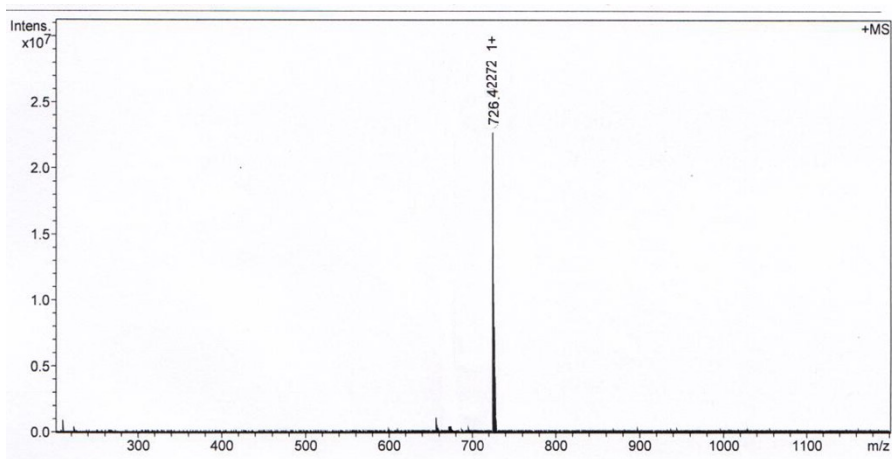

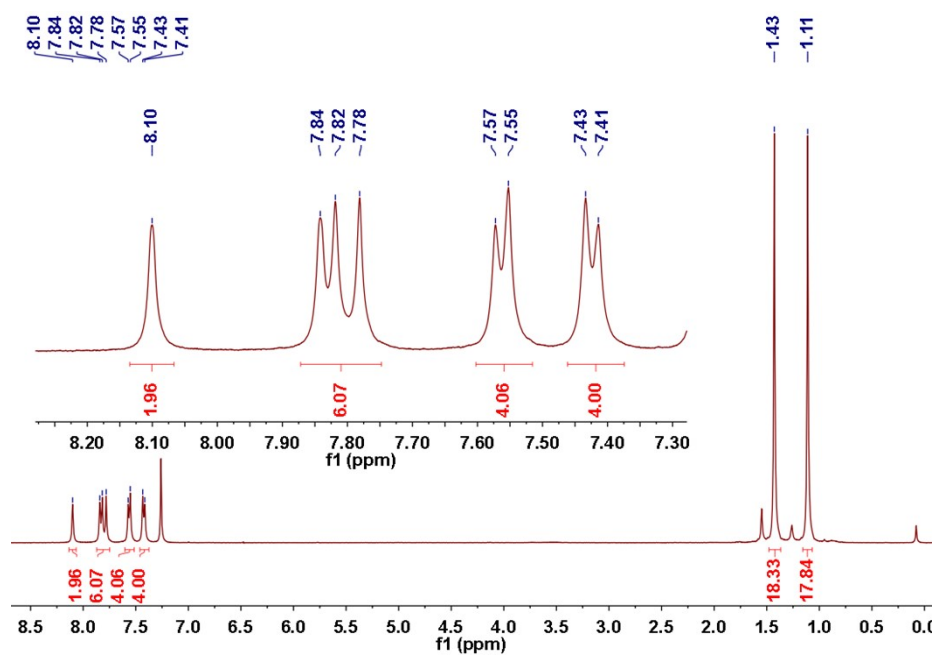**Fig. S15** ^{13}C NMR spectrum of **4**.

15

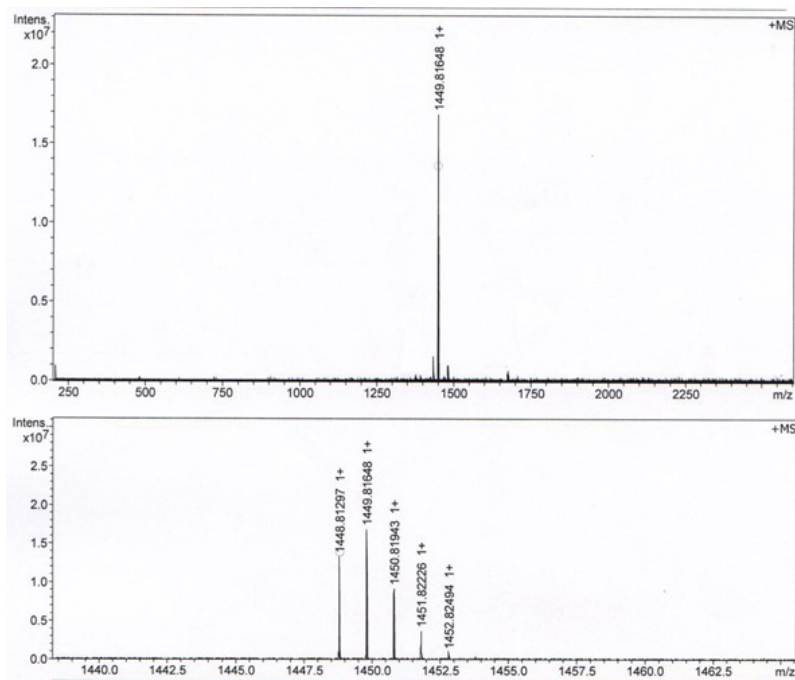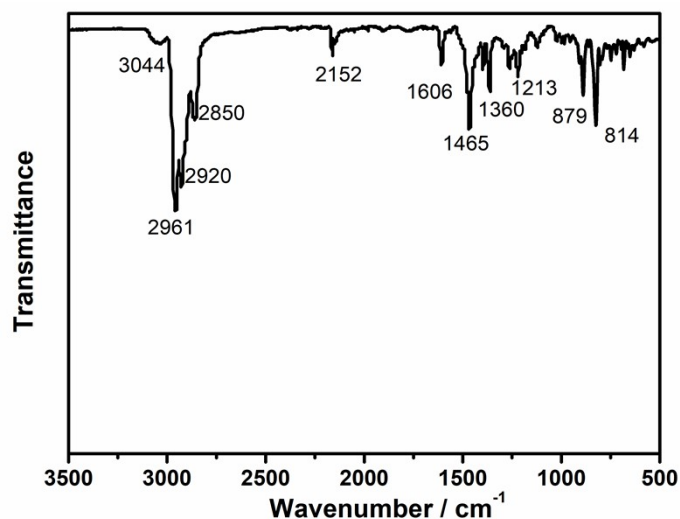**Fig. S16** MALDI-TOF spectrum of **4**

Fig. S17 ¹H NMR spectrum of **DPDD**.
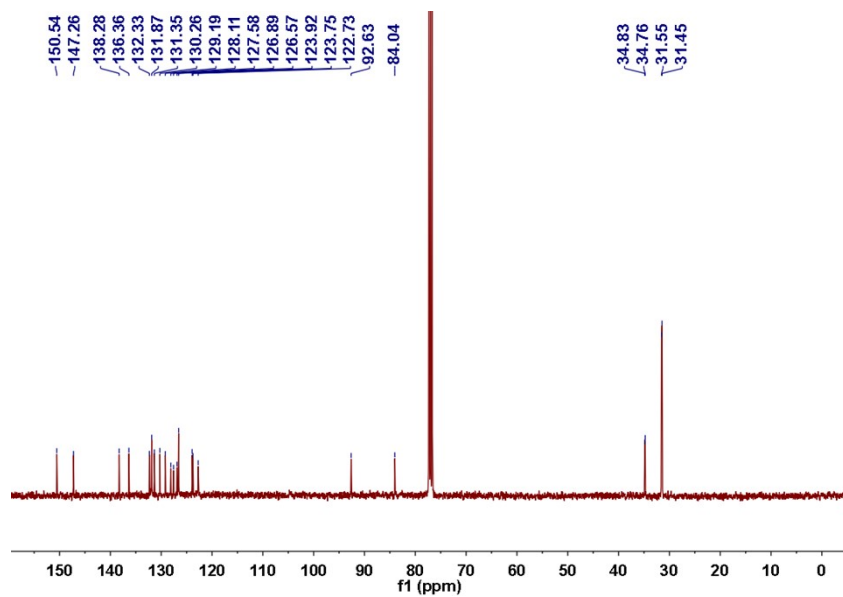
Fig. S18 ^{13}C NMR spectrum of **DPDD**.

Fig. S19 MALDI-TOF spectrum of **DPDD**.

Fig. S20 FT-IR spectrum of **DPDD**.

Notes and references

1. M. Sheik-Bahae, A. A. Said, T. H. Wei, D. J. Hagan and E. W. V. Stryland, *IEEE J. Quantum Electron.*, 1990, **26**, 760-769.

2. B. Gu, W. Ji, P. S. Patil, S. M. Dharmaprakash and H.-T. Wang, *Appl. Phys. Lett.*, 2008, **92**, 091118.

3. N. S. Makarov, M. Drobizhev and A. Rebane, *Opt. Express*, 2008, **16**, 4029-4047.

4. Robb, M. A., Cheeseman, J. R.; Scalmani, G.; Barone, V.; Mennucci, B.; Petersson,; Nakatsuji, G. A. H.; Caricato, M.; Li, X.; Hratchian, H. P.; Izmaylov,; Bloino, A. F. J.; Zheng, G. Gaussian 09, Revision B.01, Inc. Wallingford CT, 2010.